Naval Research Laboratory

Washington, DC 20375-5320

NRL/MR/6790--96-7881

Guiding of High Intensity Laser Pulses in Straight and Curved Plasma Channel Experiments

Y. Ehrlich
C. Cohen
A. Zigler

Racah Institute of Physics
Hebrew University, Jerusalem, Israel

J. Krall
P. Sprangle
E. Esarey

Beam Physics Branch
Plasma Physics Division

October 25, 1996

REPORT DOCUMENTATION PAGE

Form Approved
OMB No. 0704-0188

1. AGENCY USE ONLY (*Leave Blank*)	2. REPORT DATE	3. REPORT TYPE AND DATES COVERED
	October 25, 1996	Interim

4. TITLE AND SUBTITLE

Guiding of High Intensity Laser Pulses in Straight and Curved Plasma Channel Experiments

5. FUNDING NUMBERS

JO# 67- 7057-0-6

6. AUTHOR(S)

Y. Ehrlich, C. Cohen, A. Zigler*, J. Krall, P. Spangle, E. Esarey

7. PERFORMING ORGANIZATION NAME(S) AND ADDRESS(ES)

Naval Research Laboratory
Washington, DC 20375-5320

8. PERFORMING ORGANIZATION REPORT NUMBER

NRL/MR/6790--96-7881

9. SPONSORING/MONITORING AGENCY NAME(S) AND ADDRESS(ES)

Binational Science Foundation
Jerusalem 91076, Israel

Department of Energy
Washington, DC 20585

Office of Naval Research
Arlington, VA 22217

10. SPONSORING/MONITORING AGENCY REPORT NUMBER

11. SUPPLEMENTARY NOTES

*Racah Institute of Physics, Hebrew University, Jerusalem, Israel

12a. DISTRIBUTION/AVAILABILITY STATEMENT

Approved for public release; distribution unlimited.

12b. DISTRIBUTION CODE

13. ABSTRACT (*Maximum 200 words*)

Experimental demonstration of optical guiding of a high intensity ($> 10^{16}$ W/cm^2) laser pulse in a 1 cm long cylindrical plasma channel formed by a slow capillary discharge is presented. Optical guiding in a curved plasma (radius of curvature = 10 cm) is demonstrated for the first time. It is shown experimentally that the ($\sim 10^8$ - 10^{16} W/cm^2). Experimental results, showing guiding over approximately 11 vacuum diffraction lengths, in both straight and curved channels, are in agreement with theoretical and numerical calculations.

14. SUBJECT TERMS

Laser-plasma
Optical guiding

15. NUMBER OF PAGES

16

16. PRICE CODE

17. SECURITY CLASSIFICATION OF REPORT	18. SECURITY CLASSIFICATION OF THIS PAGE	19. SECURITY CLASSIFICATION OF ABSTRACT	20. LIMITATION OF ABSTRACT
UNCLASSIFIED	UNCLASSIFIED	UNCLASSIFIED	UL

NSN 7540-01-280-5500

Standard Form 298 (Rev. 2-89)
Prescribed by ANSI Std 239-18
298-102

GUIDING OF HIGH INTENSITY LASER PULSES IN STRAIGHT AND CURVED PLASMA CHANNEL EXPERIMENTS

Laser guiding in straight and curved plasma channels can have important applications, such as an efficient circular x-ray laser medium, optical synchrotrons, laser accelerators, and harmonic generators [1-5]. Generally, laser propagation distance is limited by diffraction and can be further limited by ionization-induced refraction [6,7]. Optical guiding is necessary to propagate the laser pulse over distances greater than the vacuum diffraction length. One approach to optical guiding of intense pulses relies on the self-induced modification of the plasma refractive index due to relativistic electron motion [8] or by ponderomotive force-driven charge displacement [9]. This approach requires high laser powers (> 1 TW). Another approach to guiding relies on a preformed plasma density channel, in which the refractive index is peaked on axis by minimizing the local ambient electron density on axis [10]. Guiding in a preformed plasma channel has been demonstrated previously [11] using two moderate intensity ($< 10^{14}$ W/cm^2) laser pulses. More recently, guiding up to ($> 10^{15}$ W/cm^2) has been demonstrated using the same technique[12]. In these experiments, the first pulse initiates a cylindrical expanding shock wave in a gas chamber to form a straight plasma channel, which guides the second pulse. Using this method, guiding has been observed over distances as large as 90 laser diffraction lengths [12]. Initial experiments on the guiding of laser pulses in one-dimension using a slab geometry capillary discharge have also been reported [13].

In this letter we report the optical guiding of a high intensity ($> 10^{16}$ W/cm^2) laser pulse over a distances of several vacuum diffraction (Rayleigh) lengths using a plasma channel formed by a slow electrical discharge in a cylindrical capillary. Using this guiding technique, we have obtained the first demonstration of guiding of a high intensity laser pulse along a curved channel.

Experimental results demonstrate that guiding takes place over a wide range of laser intensities. In these experiments, intensity was varied from $\sim 10^8$ W/cm^2 (using the oscillator only) to greater than 10^{16} W/cm^2. Results are consistent with the theoretical prediction that density channel guiding is a first-order process (unlike relativistic or ponderomotive guiding), and is independent of laser intensity [10]. The guiding distance appears to be limited only by the capillary length and absorption of the laser by the plasma. The temperature and plasma density near the capillary axis can be modified over

Manuscript approved August 23, 1996.

a wide range [14], independent of guiding conditions (channel absolute depth and width). The formation of a highly localized plasma channel by a capillary discharge in a vacuum cell enables focusing of high intensity laser pulses at the channel entrance and avoids laser propagation in a neutral gas before the laser focus. This feature is important for soft x-ray lasers, where the generated radiation can be absorbed by the neutral gas. The generated plasma consists of ions of the capillary wall material, which is made of a compound with a high concentration of hydrogen. Thus, the effective ionization state in the plasma remains almost constant even for very high laser intensities.

The ablation-dominated capillary discharge configuration, which forms the plasma channel, is shown in Fig. 1. A 1 cm long polypropylene cylinder with a 350 μm diameter hole is placed between two electrodes. The electrodes are connected to an 11 nF capacitor which is charged to 0.2 - 0.5 Joules. The discharge, which is initiated by a triggered spark-gap, has a maximum repetition rate of 1.5 Hz. The energy stored in the capacitor is ohmically dissipated in the capillary discharge and transfers energy from the capacitor to the plasma with high efficiency, since the discharge functions as a resistive element. This energy is partitioned between plasma pressure, dissociation and ionization energy, as well as kinetic energy of the plasma flow. Energy transport from the discharge to the wall, principally by radiation, causes additional ablation of the polypropylene, thereby providing additional plasma to maintain the discharge. Under conditions where the flow kinetic energy is smaller than the thermal energy, the balance between the power radiated by plasma and the input electrical power defines the plasma temperature T, capillary resistance R, and plasma density n as functions of the capillary geometry and the current I. This simple approximation yields the following scaling rules, which have been experimentally verified [14]: $T = 3.3I^{0.36}$ eV, $n = 1.3 \times 10^{20} I^{0.91}$ cm^{-3}, and $R = 1.71I^{-0.55}$ ohms, where I is in kA. Thus, the capillary plasma density and temperature can be simply controlled by varying the electrical parameters of the external circuit.

For experiments in which the capillary radius was smaller than Rosseland[15] mean free path, which governs the radiation losses, the radial electron density profile was found to be parabolic, with a minimum on axis [16]. The parabolic profile is the result of the radial profiles of the pressure and temperature. The pressure across the capillary is expected

to be constant, since any disturbance in the radial direction will equilibrate with a time scale given by the capillary radius divided by the sound speed. This time scale is much shorter than both the discharge duration ($\sim$ 1 μsec) and the plasma flow time along the channel. In addition, the temperature is higher at the center and drops near the wall, due to radiation and collisional heat transfer. Therefore, the density is minimum on axis and increases towards the capillary walls. In this experiment and in Ref. [16], the axial plasma temperature was $\sim$ 3 eV and the electron density varied within the range $\sim (1-5)\times 10^{19}$ cm^{-3}.

For a parabolic plasma channel of the form $n = n_0 + \Delta n r^2/r_{ch}^2$, where r_{ch} is the radius of the plasma channel, it can be shown [10] that a laser pulse with a radial profile $\sim \exp(-r^2/r_L^2)$ will be matched ($dr_L/dz = 0$) within the channel with a laser spot size (radius) $r_L = r_M$ given by $r_M = [r_{ch}^2/(\pi r_e \Delta n)]^{1/4}$, where $r_e = e^2/mc^2$ is the classical electron radius. For representative parameters, $r_{ch} = 150$ μm and $n_0 \simeq \Delta n = 4\times 10^{18}$ cm^{-3}, the matched beam radius is $r_M = 28$ μm.

Since the capillary discharge typically produces a large-radius channel ($r_{ch} > 100$ μm), it is capable of transmitting a wide range of laser spot sizes. At one extreme, a laser with $r_L = r_{ch} = 150$ μm can be guided with a density depression of $\Delta n/n < 1\%$. In addition, the capillary discharge can produce a large density depression ($\Delta n > 10^{19}$ cm^{-3}), so that tightly-focused laser pulses ($r_L < 10$ μm) can be guided.

The propagation experiments were carried out using a 1 cm long straight cylindrical polypropylene capillary tube with an inner diameter of 350 μm, as well as a curved capillary tube, with length 1 cm, inner diameter 350 μm and having a 10 cm radius of curvature.

The experiments were conducted using the Hebrew University Laser which consists of a Ti-Sapphire oscillator followed by regenerative and four-pass amplifiers. The system is capable of delivering a linearly-polarized, 100 fs pulse with energy up to 50 mJ at wavelength $\lambda = 0.80$ μm with repetition rate of 10 Hz. Timing electronics that trigger both the laser and the spark-gap allow synchronization of the laser pulse arrival and the discharge initiation. Using this technique, we were able to vary the delay between the initiation of the electrical discharge and the arrival of the laser pulse.

The laser was focused on the capillary channel by means an $F^{\#} = 11.5$ lens, which

produces a laser waist $r_{L0} \simeq 15$ μm when focused in vacuum. The minimum spot size of 15 μm implies that the beam is ~1.6 times the diffraction-limited value of $\lambda F^{\#} \simeq 9.2$ μm [17]. Operating at pulse energy 4 mJ, the peak focused intensity was $\sim 10^{16}$ W/cm^2. The capillary was located in a 10^{-4} torr vacuum chamber, with the capillary entrance placed at the focal plane of the laser focusing lens. The alignment of the delivery and collecting optics, outside the vacuum chamber, was achieved with a 1 mW He-Ne laser. The final angular and transverse positioning of the optics system was performed using the Ti-Sapphire oscillator.

The input and transmitted laser energy in the capillary was measured by splitting and focusing a portion of the beam into two calibrated photo-diodes (see Fig. 1). Photo-Diode 1 provides input data, including laser energy and timing. Photo-Diode 2 measures the amount of laser light transmitted through the capillary. The laser light transmitted through the plasma channel was collected and imaged by an optical system onto a CCD camera. The imaged intensity was reduced by inserting thin calibrated neutral density filters. The beam interference in these filters is responsible for the beam profile modulation seen in Figs. 2 and 3. These figures show single-shot images of the laser beam at the capillary exit, recorded at 10 Hz by the CCD camera with and without the discharge for the straight (Fig. 2) and curved (Fig. 3) capillary tubes. The difference between the maximum discharge repetition rate (1.5 Hz) and laser repetition rate (10 Hz), allows comparison of the guided and unguided laser pulse images under otherwise identical conditions. Figures 2 and 3 show guiding over a distance $\simeq 11 Z_{R0}$, where $Z_{R0} = \pi r_{L0}^2/\lambda = 0.088$ cm is the Rayleigh length.

The laser beam expansion after passing through the capillary channel was measured by recording the images of the transmitted light at various locations. Measurements were taken at distances between 0 and 1 cm from the capillary exit. In the case of the straight capillary, the focusing and collecting optics were placed on the same optical axis. In the curved capillary experiments the optical systems were placed at an angle of 3° relative to the channel axis (6° between the two optical systems axes).

Experimental results show substantial increases in the laser energy transmission and a substantial reduction of the laser spot size at the capillary exit when the capillary is

discharged. When the laser pulse (focused using an $F^{\#} = 11.5$ lens) was transmitted through the straight capillary without an electrical discharge, the energy transmission was 25%. This value corresponds to the geometrical opening of the capillary and indicates very low reflection at the capillary walls (the radius of the transmitted laser light at the capillary exit was equal to the capillary radius of 175 μm). When the pulse is focused at the capillary entrance 250 ns after initiation of the electrical discharge, the typical energy transmission increases to 75% and the emerging pulse radius is reduced to 30 μm (Fig. 2). Experimental results indicate a critical sensitivity to alignment and timing between initiation of the discharge and the arrival of the laser pulse. Enhanced capillary transmission is obtained for laser pulses injected 200 ns to 350 ns after the discharge is initiated. For shorter delays, no significant effect was observed. For longer delays, the spot size of the transmitted pulse remains small (as in optimal case), but the amount of the transmitted light is reduced.

Performance as a function of stored electrical energy was studied in the straight capillary geometry by using two capacitors for the electrical discharge: 2.1 nF and 11 nF and by varying the voltage across the capillary. However, voltage variation also affects the plasma density according to the scaling rules stated earlier. Optimal guiding was obtained using the 2.1 nF capacitor and a discharge voltage of 13 kV. For these values, the maximum current was 500 A. Using the 2.1 nF capacitor, capillary wall erosion was found to be relatively small. There was no significant widening of the capillary channel after 100 shots. For discharge voltages significantly above 15 kV, the transmitted laser intensity was negligible; at low voltages, the guiding was less pronounced. The transmitted laser pulse outside the capillary was monitored at various distances from the capillary exit. Measurements of the beam diameter were obtained by varying the distance between the capillary exit and the focal plane of the collecting optical system. It was found that the laser pulse spot size did not vary significantly at distances from 2 mm to 7 mm away from the capillary exit. Small variations in the spot size were attributed to variations in Δn consistent with recent simulation results and possibly jitter in the timing between the initiation of the discharge and the pulse arrival. In addition, plane imaging was used to measure the beam profile at several positions after the exit of the capillary tube in the same shot. For this purpose, five beam splitters were placed between the imaging lens and the CCD camera. The image

taken by each beam splitter shows the laser radial profile at a particular position. Beam radial profile data were taken at distances 0, 0.2, 0.4, 0.6 and 0.8 cm from the exit of the capillary. A beam divergence angle of $\gtrsim 8$ mrad was found.

Figure 3 shows the results of optical guiding experiments along a curved plasma channel using the 11 nF capacitor and a discharge voltage of 9.3 kV. In the curved channel experiments, capillary performance was sensitive to the alignment of the the laser beam with respect to the capillary axis. With optimal alignment and a 10 cm radius-of-curvature plasma channel, energy transmission was as high as 85%, and the laser spot radius at the capillary exit was 50 μm. In experiments using a capillary having a 4.2 cm radius of curvature (other parameters identical), the peak energy transmission was ~2%, in good agreement theory (see below).

To examine propagation of the laser pulse into, through, and out of the straight channel, simulations were performed using the 2D (r, z) LEM nonlinear laser code [18]. Figure 4 shows the laser spot radius r_L plotted versus propagation distance z through the channel, which is located at $0.5 < z < 1.5$ cm. In the simulation, the on-axis plasma density is 5.0×10^{18} cm^{-3}, $\Delta n = 4.0 \times 10^{18}$ cm^{-3}, and $r_{ch} = 150$ μm. The laser pulse is focused at the channel entrance with a minimum spot size $r_{L0} = 15$ μm. Since the experimental spot size is 1.6 times the diffraction-limited value, the simulation code was heuristically modified to reduce the vacuum diffraction length by this same factor. Figure 4 shows that the laser spot radius oscillates about the matched beam radius $r_M = 28$ μm as it is guided through the 1 cm long channel. For comparison to the guided case, laser propagation in vacuum (no channel) is also shown. At the capillary exit, the laser spot radius is 45 μm and the divergence angle is $\simeq 14$ mrad, in good agreement with experiment.

Laser propagation in a curved plasma channel can be analyzed in the low-laser-intensity limit. In this limit, nonlinear (relativistic and ponderomotive) effects are neglected and the channel is assumed to be unaffected by the laser pulse. In a straight channel, the laser electric field, $E = \frac{1}{2}\hat{E}e^{ik(z-ct)} + c.c.$, obeys the paraxial wave equation

$$\left(\nabla_\perp^2 + 2ik\partial/\partial z\right)\hat{E} = k^2\left(1-\eta^2\right)\hat{E}, \tag{1}$$

where $\omega = ck$ is the laser frequency, z is along the channel axis, η is the index of refraction,

c.c. denotes the complex conjugate, and $|\partial\hat{E}/\partial z| \ll k|\hat{E}|$ is assumed. The linear index of refraction for a plasma is given by $\eta \simeq 1-\omega_p^2/2\omega^2$, where $\omega_p = (4\pi e^2 n/m)^{1/2}$ is the plasma frequency and n is the plasma density.

Consider a channel which is curved in the (x,z) plane with a constant radius of curvature R_0, where z is the distance along the curved channel axis and x, y, and $r = (x^2+y^2)^{1/2}$ are defined with respect the the channel axis. It can be shown that the paraxial wave operator in the curved coordinate system becomes $(\nabla_\perp^2+2ik\partial/\partial z+2k^2x/R_0)\hat{E}$ where $\nabla_\perp^2 = \partial^2/\partial x^2 + \partial^2/\partial y^2$ and higher order terms (smaller by at least $r/R_0 \ll 1$) have been neglected. Hence, the laser field envelope, $\hat{E}$, obeys the paraxial wave equation, Eq. (1), with an effective index of refraction given by

$$\eta_{eff} = 1 - \omega_p^2(r)/2\omega^2 + x/R_0, \tag{2}$$

where the x/R_0 term represents the effects of curvature. Assuming a density channel of the form $n = n_0 + \Delta n r^2/r_{ch}^2$, it can be shown that the solution to Eq. (1) with $\eta = \eta_{eff}$ is given by

$$\hat{E} = E_0 \exp\left[i\Delta k z + ik_x(x-x_c) - (x-x_c)^2/r_0^2 - y^2/r_0^2\right], \tag{3}$$

where r_0 is the matched laser spot radius given by $r_0^4 = r_{ch}^2/(\pi r_e \Delta n)$, Δk is the wave number shift, $k_x = k\partial x_c/\partial z$, and the laser pulse centroid x_c satisfies

$$\partial^2 x_c/\partial z^2 + x_c/Z_{R0}^2 = 1/R_0, \tag{4}$$

where $Z_{R0} = kr_0^2/2$ is the Rayleigh length of the matched beam. In Eq. (3), Δk represents a small phase shift given by $\Delta k = -[\omega_p^2/(2c^2k^2)+2/(r_0k)^2-k_x^2/(2k^2)+x_c^2/(r_0^4k^2)-x_c/R_0]k$, where $|\Delta k| \ll k$. Equation (4) indicates that the laser centroid x_c oscillates in z about an equilibrium offset value given by $x_{c0} = Z_{R0}^2/R_0$. Clearly this offset must be less than the channel radius or the laser will be lost from the channel. This sets a minimum acceptable radius of curvature:

$$R_0 \geq Z_{R0}^2/r_{ch}. \tag{5}$$

For a matched beam ($r_0 = 28$ μm) and representative experimental parameters ($\lambda = 0.8$ μm and $r_{ch} = 150$ μm), $Z_{R0} = 0.31$ cm and $R_0 \geq 6.4$ cm. This value is in excellent agreement with the experimental results.

In summary, optical guiding of high intensity ($> 10^{16}$ W/cm^2) laser pulses has been demonstrated using both straight and curved channel geometries, where the plasma channel is formed by a slow cylindrical capillary discharge. Results, which demonstrate guiding of $\gtrsim 75\%$ of the laser pulse energy over a distance of $\simeq 11$ Rayleigh lengths, are in good agreement with theoretical and numerical calculations.

This work was supported by the US-Israeli Binational Science Foundation, the U.S. Office of Naval Research, and the U.S. Department of Energy.

References

[1] See, e.g., *Special Issue on Plasma Based Accelerators*, ed. by T. Katsouleas and R. Bingham, IEEE Trans. Plasma Sci. **24**, pp. 249-460 (1996); C.E. Clayton et al., Phys. Rev. Lett. **70**, 37 (1993); K. Nakajima et al., Phys. Rev. Lett. **74**, 4428 (1995); A. Modena et al., Nature **337**, 606 (1995).

[2] P. Sprangle et al., Appl. Phys. Lett. **53**, 2146 (1988); E. Esarey et al., Phys. Fluids B **5**, 2690 (1993).

[3] H. Milchberg, C. Durfee, and J. Lynch, J. Opt. Soc. Am. B **12**, 731 (1995).

[4] J. Macklin, J. Kmetec, and C. Gordon, Phys. Rev. Lett. **70**, 760, (1993).

[5] P. Eisenberger and S. Suckewer, Science **273** (in press).

[6] P. Sprangle et al., to appear in Phys. Rev. E (1996).

[7] W.P. Leemans et al., Phys. Rev. A **46**, 1091 (1992).

[8] C.E Max, J. Arons, and A.B Langdon, Phys. Rev. Lett. **33**, 209 (1974); P. Sprangle, C.M. Tang, and E. Esarey, IEEE Trans. Plasma Sci. **PS-15**, 145 (1987).

[9] G.Z. Sun et al., Phys. Fluids **30**, 526 (1987); A.B. Borisov et al., Phys. Rev. A **45**, 5830 (1992).

[10] P. Sprangle and E. Esarey, Phys. Fluids B **4**, 2241 (1992); P. Sprangle et al., Phys. Rev. Lett. **69**, 2200 (1992); E. Esarey, J. Krall, and P. Sprangle, Phys. Rev. Lett. **72**, 2887 (1994).

[11] C. Durfee and H. Milchberg, Phys. Rev. Lett. **71**, 2409 (1993); C. Durfee, J. Lynch, and H. Milchberg, Phys. Rev. E **51**, 2368 (1995).

[12] H. M. Milchberg et al., Phys. Plasmas **3**, 2149 (1996).

[13] A. Zigler et al., J. Opt. Soc. Am. B **13**, 68 (1996).

[14] A. Loeb and Z. Kaplan, IEEE Trans. Magn. **25**, 342 (1989); R. Burton et al., IEEE Trans. Plasma Sci. **19**, 340 (1991); Y. Ehrlich et al., Appl. Phys. Lett. **64**, 3542 (1994).

[15] Ya. B. Zel'dovich and Yu. P. Razier, *Physics of Shock Waves and High Temperature Hydrodynamic Phenomena* (Academic Press, New York, 1966).

[16] J. Ashkenazy, R. Kipper, and M. Caner, Phys. Rev. A **43**, 5568 (1991); B. Brill et

al., J. Phys. D **23**, 1064 (1990); A. Loeb and Z. Kaplan, IEEE Trans. Magn. **25**, 342 (1989); E. Lithman, M.Sc. Thesis, Hebrew Univ. (1995).

[17] A. E. Seigman, *Lasers* (University Science Books, Mill Valley, California, 1986), p 676.

[18] J. Krall et al., Phys. Plasmas **1**, 1738 (1994).

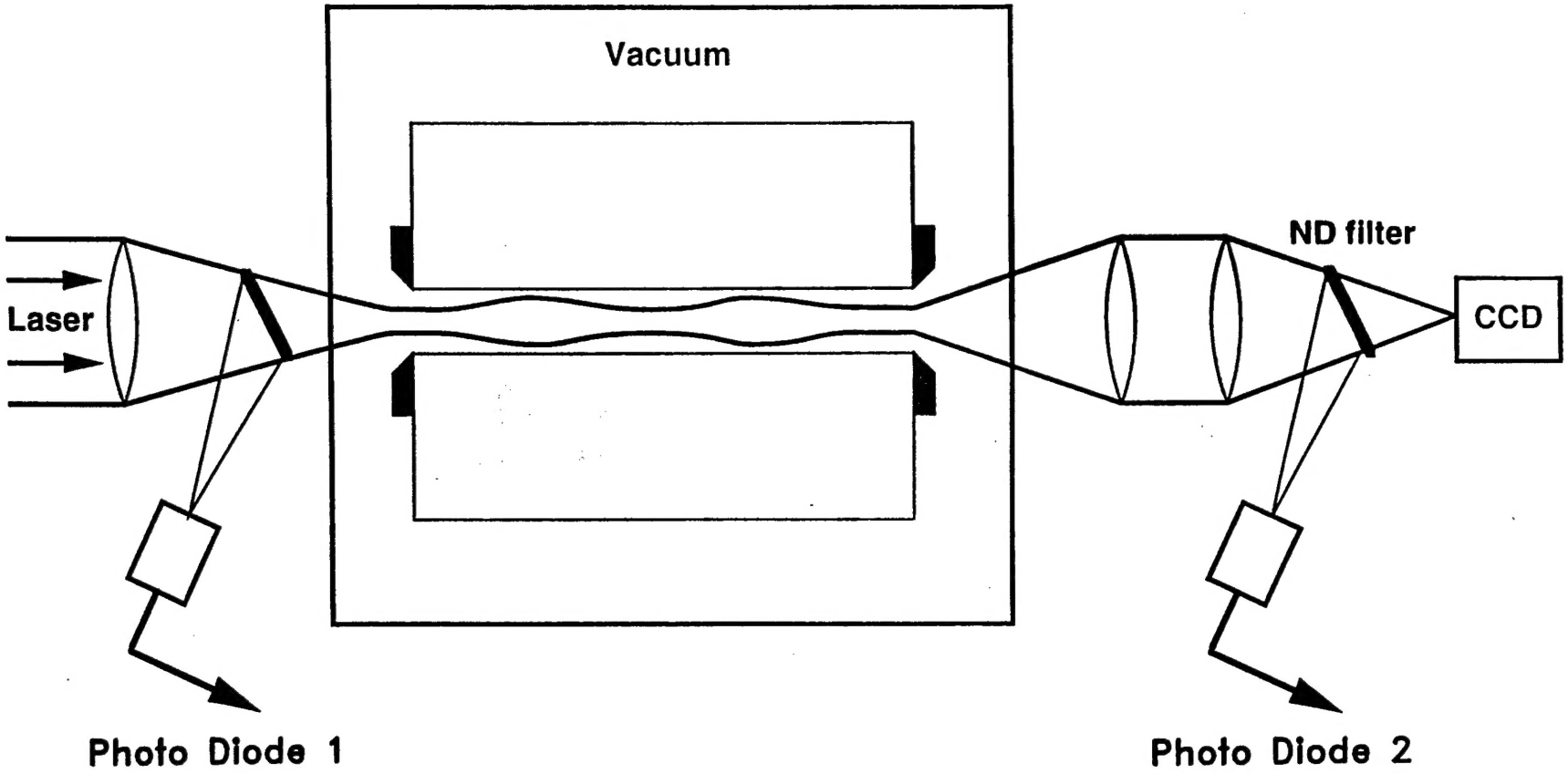

Fig. 1. Experimental set-up.

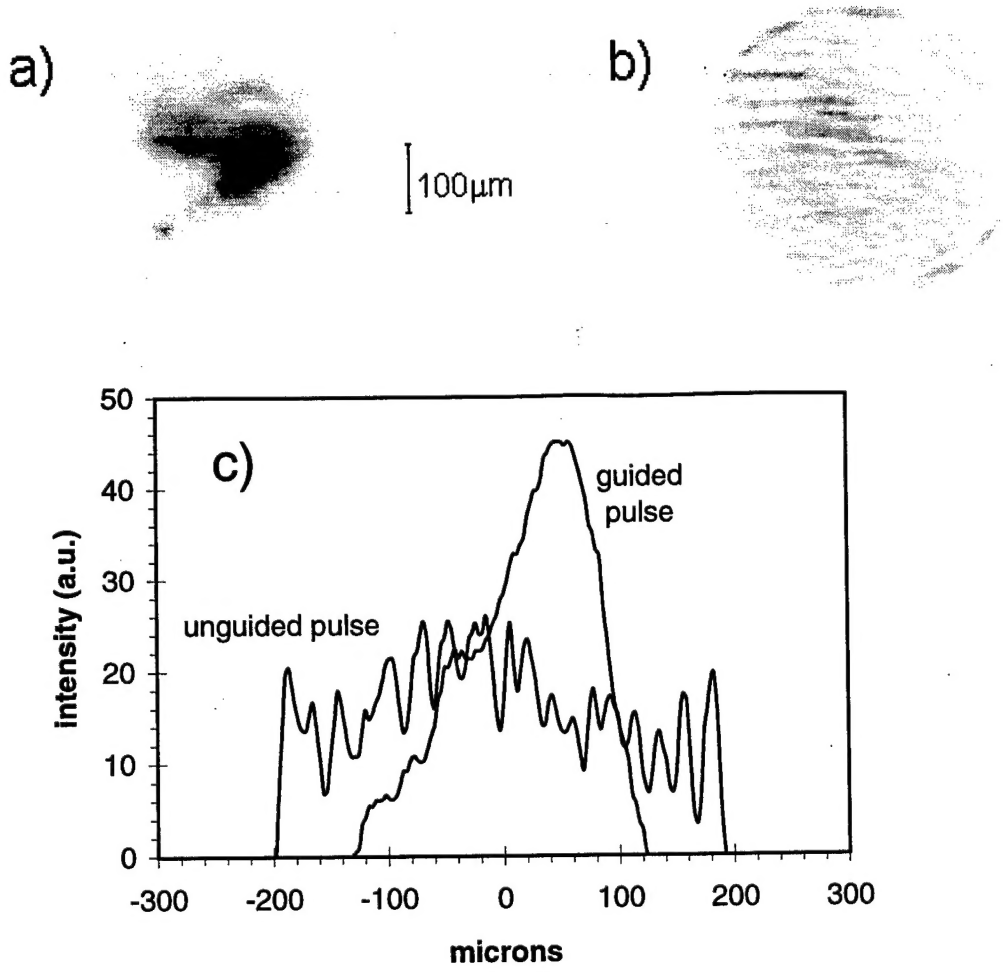

Fig. 2. C.C.D. images of the laser pulse emerging from the straight capillary for (a) a guided pulse and (b) an unguided pulse. Intensity profiles (c) from the images are also shown. Note that the focal plane is 2 mm from the capillary exit and that the interference lines are due to low grade neutral density filters.

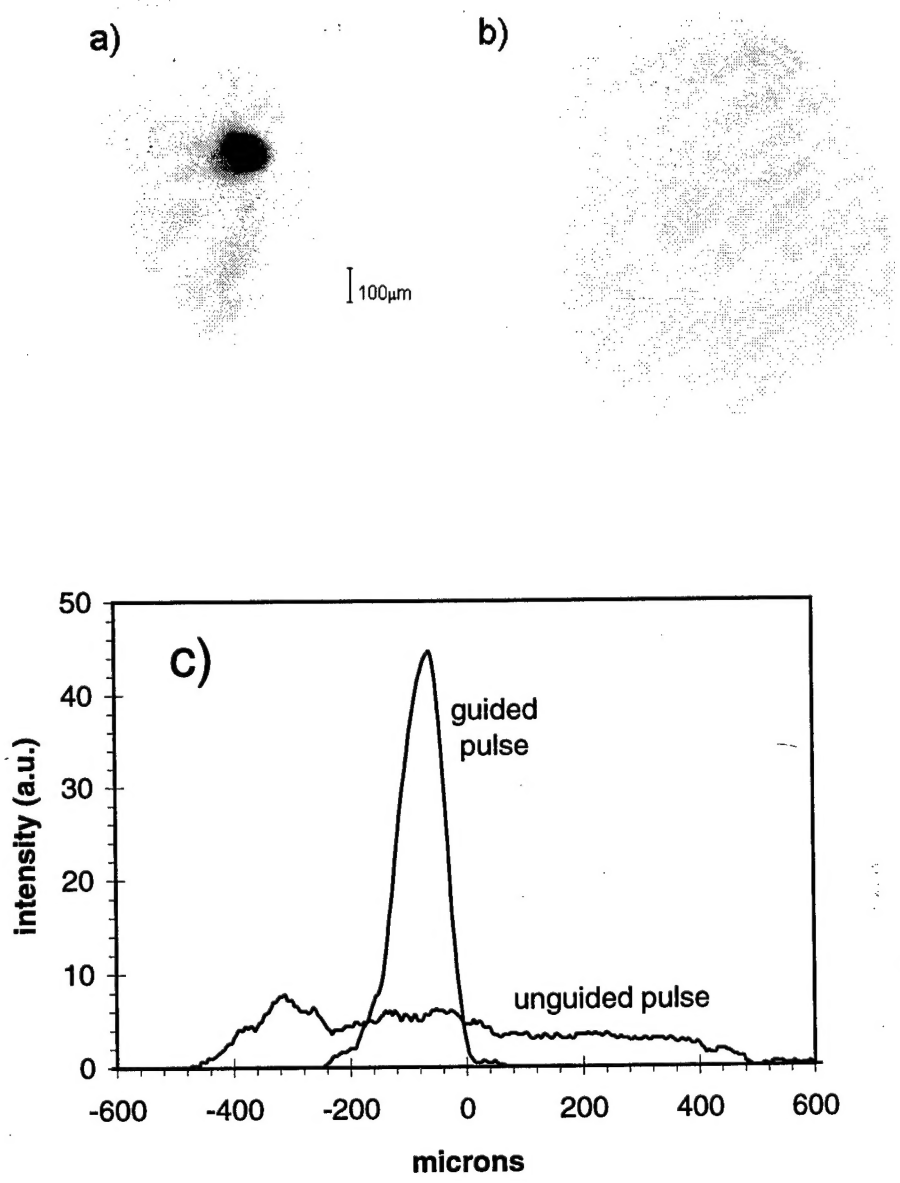

Fig. 3. C.C.D. images of the laser pulse emerging from the curved capillary (radius of curvature 10 cm) for (a) a guided pulse and (b) an unguided pulse. Intensity profiles (c) from the images are also shown. The focal plane is 5 mm from the capillary exit.